HYDROELASTIC RESPONSE OF FLOATING JETTY AT KRABI, THAILAND

C. M. Wang[1,2*], R. P. Gao[1,2†], and M. M. Pathak[1]

[1]*Department of Civil and Environmental Engineering, National University of Singapore, Singapore*
[2]*Engineering Science Programme, National University of Singapore, Singapore*

ABSTRACT

This paper presents a study on the hydroelastic response of the floating jetty at Krabi, Thailand which has been observed to be rather large under wave action. In the hydroelastic analysis, the floating jetty is modeled as a longish isotropic sandwich plate according to the Mindlin plate theory. The water is assumed to be an ideal fluid and its motion is irrotational so that a velocity potential exist. In order to decouple the fluid–structure interaction problem, the modal expansion method is adopted for the hydroelastic analysis which is carried out in the frequency domain. The boundary element method is used to solve the Laplace equation for the velocity potential, whereas the finite element method is employed for solving the equations of motion of the floating plate. Hydroelastic behaviors of the Krabi floating jetty were investigated by experimenting with different materials and connector systems. The results show that the hydroelastic response of the floating jetty is greatly affected by the type of material and connector system used. By choosing an appropriate material and a suitable connector system, the hydroelastic response of the Krabi floating jetty can be reduced significantly.

Keywords: Floating jetty, hydroelastic response, sandwich plate, connector system

1. INTRODUCTION

Pontoon-type, very large floating structures (VLFS) have been used for applications like floating bridges and floating jetties. When subjected to wave actions, these flexible floating structures exhibit hydroelastic deformations. An example is the response of the floating jetty found in Krabi, Thailand under wave action as shown in Fig. 1. Its hydroelastic response is so large that it is unsafe for people to walk on. Triggered by this observation, we simulate the hydroelastic behavior of the Krabi floating jetty and study ways to mitigate its large hydroelastic response by using different materials and connector systems.

Figure 1: Krabi's floating jetty.

* Presenter: Email: ceewcm@nus.edu.sg
† Corresponding author: Email: gaoruiping@nus.edu.sg

2. HYDROELASTIC ANALYSIS IN FREQUENCY DOMAIN

2.1. Water–plate model

The floating jetty can be considered as a flat longish plate of length L, width B, height h, and with a zero draft. It floats on water of constant depth H. The water is assumed to be an ideal fluid (inviscid and incompressible), and its flow is irrotational. The free and undisturbed water surface is at $z = 0$ while the seabed is found at $z = -H$. By assuming an incident wave ϕ_I with a circular frequency ω, wavelength λ and wave height $2A$ that enters the computational domain, the water motion and plate deflection will undergo a steady state harmonic motion with the same frequency ω. The deflection w of the plate is measured from the free and undisturbed water surface. Figure 2 shows the floating jetty model, where $k_{rj} = \zeta_{rj}D/L$ (j = 1,2, …, n_c) is the constant for the j-th rotational spring, D is the flexural rigidity of the plate and n_c is the number of connections used.

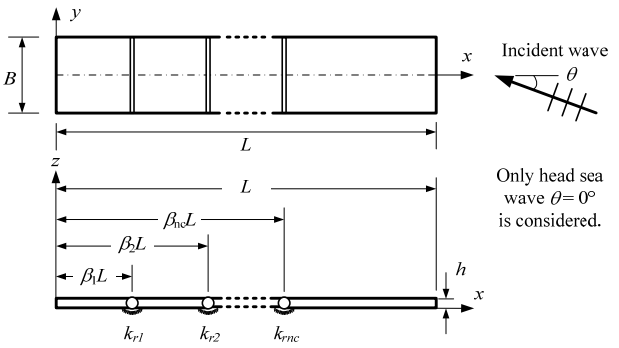

Figure 2: Floating jetty model.

2.2. Equations of motion for floating plate

The floating jetty is modeled as an isotropic and elastic sandwich plate based on the Mindlin plate theory (Liew et al. 1998). The motion of the Mindlin plate is represented by the vertical displacement $w(x,y)$, the rotation $\psi_x(x,y)$ about the y-axis and the rotation $\psi_y(x,y)$ about the x-axis. The governing equations of motion for the Mindlin plate (after omitting the time factor $e^{-i\omega t}$) are

$$\kappa^2 Gh\left[\left(\frac{\partial^2 w}{\partial x^2}+\frac{\partial^2 w}{\partial y^2}\right)+\left(\frac{\partial \psi_x}{\partial x}+\frac{\partial \psi_y}{\partial y}\right)\right]+\rho_p h\omega^2 w = p(x,y) \tag{1a}$$

$$D\left[\frac{(1-\nu)}{2}\left(\frac{\partial^2 \psi_x}{\partial x^2}+\frac{\partial^2 \psi_x}{\partial y^2}\right)+\frac{(1+\nu)}{2}\left(\frac{\partial^2 \psi_x}{\partial x^2}+\frac{\partial^2 \psi_y}{\partial x \partial y}\right)\right]-\kappa^2 Gh\left(\frac{\partial w}{\partial x}+\psi_x\right)+\rho_p \frac{h^3}{12}\omega^2 \psi_x = 0 \tag{1b}$$

$$D\left[\frac{(1-\nu)}{2}\left(\frac{\partial^2 \psi_y}{\partial y^2}+\frac{\partial^2 \psi_y}{\partial x^2}\right)+\frac{(1+\nu)}{2}\left(\frac{\partial^2 \psi_y}{\partial y^2}+\frac{\partial^2 \psi_x}{\partial x \partial y}\right)\right]-\kappa^2 Gh\left(\frac{\partial w}{\partial y}+\psi_y\right)+\rho_p \frac{h^3}{12}\omega^2 \psi_y = 0 \tag{1c}$$

where $G = E/[2(1+\nu)]$ is the shear modulus, κ^2 the shear correction factor taken as 5/6, ρ_p the mass density of the plate, h the thickness of the plate, $D = Eh^3/\left[12\left(1-\nu^2\right)\right]$ the flexural rigidity, E the Young's modulus and ν the Poisson ratio. The pressure $p(x,y)$ in Eq. (1a) comprises the hydrostatic and hydrodynamic pressure, i.e.

$$p(x,y) = -\rho g w + i\omega\rho\phi(x,y,0) \tag{2}$$

where ρ is the mass density of water, i the imaginary number ($i = \sqrt{-1}$), g the gravitational acceleration and $\phi(x,y,0)$ the velocity potential of water on undisturbed water surface.

When considering a sandwich plate that has a core and two facing sheets at the top and bottom, the flexural rigidity D, shear modulus G, Poisson's ratio v, and the density ρ_p of the sandwich plate can be expressed as (Liew et al. 1998)

$$D = D_c + D_f, \quad G = \frac{G_c h_c + 2G_f h_f}{h_c + h_f}, \quad \nu = \frac{\nu_c D_c + \nu_f D_f}{D_c + D_f}, \quad \rho_p = \frac{\rho_c h_c + 2\rho_f h_f}{h_c + 2h_f} \tag{3}$$

where subscripts c and f denotes core and facing, respectively. $D_c = E_c I_c / \left(1-\nu_c^2\right)$ is the flexural rigidity of the core, $D_f = E_f I_f / \left(1-\nu_f^2\right)$ the flexural rigidity of the facing, $G_c = E_c / \left[2\left(1+\nu_c\right)\right]$ the shear modulus of the core, $G_f = E_f / \left[2\left(1+\nu_f\right)\right]$ the shear modulus of the facing, $I_c = h_c^3 / 12$ the moment of area of the core per unit width and $I_f = \frac{2}{3} h_f \left(h_f^2 + \frac{3h_c^2}{4} + \frac{3h_c h_f}{2} \right)$ the moment of area of the facing sheet per unit width.

2.3. Equations of motion for water

By adopting the linear potential wave theory, the single frequency velocity potential of water must satisfy the Laplace's equation (Sarpkaya and Isaacson 1981)

$$\nabla^2 \phi(x, y, z) = 0 \tag{4}$$

The velocity potential ϕ of water can be separated into the three parts as (Eatock Taylor and Waite 1978, Newman 1994)

$$\phi\left(x, y, z\right) = \phi_I\left(x, y, z\right) + \phi_S\left(x, y, z\right) + \phi_R\left(x, y, z\right) \tag{5}$$

where ϕ_I, ϕ_S and ϕ_R are incident, scattering and radiation potentials, respectively. The incident potential ϕ_I can be expressed by an analytical expression whereas the scattering potential ϕ_S and the radiation potential ϕ_R can be determined by using the boundary element method (Wang et al. 2008). At the fluid–structure interface, the following boundary conditions are imposed:

$$\frac{\partial \phi_S}{\partial z}\left(x, y, 0\right) = -\frac{\partial \phi_I}{\partial z}\left(x, y, 0\right), \text{ and } \frac{\partial \phi_R}{\partial z}\left(x, y, 0\right) = -i\omega w \tag{6a, b}$$

2.4. Decoupling the equations and hydrodynamic analysis

Equations (1a), (2) and (6b) indicate that the response of the floating structure is coupled with the fluid motion (or the velocity potential). In order to decouple this fluid-structure interaction problem, the modal expansion method (Eatock Taylor and Waite 1978, Newman 1994) is adopted. In this method, the deflection of the plate $w(x,y)$ is expanded by N series of products of the modal function $c_l^w(x,y)$ and the complex amplitudes ς_l^w as

$$w\left(x, y\right) = \sum_{l=1}^{N} \varsigma_l^w c_l^w\left(x, y\right) \tag{7}$$

Similarly, the radiation potential ϕ_R is expanded as

$$\phi_R\left(x, y, z\right) = \sum_{l=1}^{N} \varsigma_l^\phi \phi_l\left(x, y, z\right) \tag{8}$$

By assuming that the complex amplitudes ς_l^w are the same as ς_l^ϕ (Eatock Taylor and Waite 1978, Newman 1994), the interaction (Eq. (6b)) at the fluid–structure interface can be decoupled as

$$\frac{\partial \phi_l}{\partial z}(x,y,0) = -i\omega c_l^w \tag{9}$$

where the modal function $c_l^w(x,y)$ can be obtained from a free vibration analysis of the plate.

After decoupling the interaction, the governing equation of motion of the fluid together with appropriate boundary conditions can be transformed into a boundary integral equation by applying the Green's second identity (Wang et al. 2008). The resulting boundary integral equation is

$$\phi_l(\mathbf{x}) + \int_{S_{HB}} \frac{\partial G(\mathbf{x},\boldsymbol{\xi})}{\partial z} \phi_l(\boldsymbol{\xi})\, d\xi = \begin{cases} \int_{S_{HB}} -i\omega G(\mathbf{x},\boldsymbol{\xi}) c_l^w(\boldsymbol{\xi})\, d\xi & \text{for } l = 1,2,\ldots,N \\ 4\pi\phi_I & \text{for } l = D \end{cases} \tag{10}$$

where $\mathbf{x} = (x,y,z)$ is the source point and $\boldsymbol{\xi} = (\xi,\eta,\zeta)$ the field point. $G(\mathbf{x},\boldsymbol{\xi})$ is a free-surface Green's function for water of finite depth that satisfies the sea bed boundary condition, water free surface boundary condition and boundary at infinity (Linton 1999). By using such a Green fucntion, only the wetted bottom surface (S_{HB}) of the floating plate needs to be considered in the analysis.

2.5. Solution of the plate-water equations

By solving the boundary integral equation (10) using the Green's function, the radiated potential ϕ_R and diffracted potential ϕ_D (= $\phi_I + \phi_S$) can be obtained. Thus, the pressure (Eq. (2)) acting on the floating body can be computed. Finally, by substituting this pressure into the plate equation (1), the coupled plate–water linear equation can be obtained as

$$[c]^T_{N\times q}\left([K_f]+[K_s]+[K_w]-\omega^2[M]-\omega^2[M_w]-i\omega[C_w]\right)_{q\times q}[c]_{q\times N}\{\varsigma\}_{N\times 1} = [c]^T_{N\times q}\{F\}_{q\times 1} \tag{11}$$

where $[K_f]$, $[K_s]$, $[K_w]$, $[M]$, $[M_w]$, $[C_w]$ and $\{F\}$ are the global flexural stiffness matrix, global shear stiffness matrix, global hydrostatic stiffness matrix, global mass matrix, global added mass matrix, global added damping matrix, and global force vector respectively. The subscripts in Eq. (11) denote the size of the matrix, where q is the total number of degrees of freedom in the plate domain and N the number of vibration modes. The modal function $[c]$ contains the eigenvectors corresponding to the plate deflection and rotations. Upon solving the coupled plate–water Eq. (11), we obtain the complex amplitudes $\{\varsigma\}$ and then we back-substitute the amplitudes into Eq. (7) to obtain the deflection and rotations of the plate $\{w, \psi_x, \psi_y\}$.

3. RESULTS AND DISCUSSION

The validity and accuracy of the present formulation with a flexible line connector have been established by Gao et al. (2011). However, in the case of multiple hinge connectors, the number of rigid body modes increases with respect to the number of hinge connectors. Therefore, sufficient modes should be considered in the modal expansion method for convergence (Lee and Newman 2000). Based on a convergence study, the total number of modes is set to $N = 400$ for present study

in the case of multiple hinge connections.

A dimensionless deflection parameter Ψ, that indicates the displacement volume of the plate, is adopted to quantify the hydroelastic response of the floating jetty. This parameter is defined as

$$\Psi = \frac{1}{ABL}\int_0^L \int_{-B/2}^{B/2} |w| \, dydx \tag{12}$$

In this section, we first simulate the response of the Krabi floating jetty by using the model discussed in Section 2. The actual response of the jetty observed from a video (Savannah 2011) will be compared with the present numerical results. The influence of boundary conditions at the jetty's front end will also be studied. Next, we examine the effect of different facing materials and connectors on the response of the jetty.

Table 1. Details of floating plate model

Parameter	Symbol	Unit	Value
Total length	L	m	164
Total width	B	m	4
Total height	h	m	0.390
Thickness of facings	h_f	mm	see Table 2
Thickness of core	h_c	mm	see Table 2
Number of connections	n_c		339
Connections location	$\beta_1 L$	m	0.483
Connection rotational stiffness coefficient	ζ_r		0(hinge), 6(semi-rigid), 600(rigid)
Water depth	H	m	20
Wave period	T	s	4
Wave height	$2A$	m	1
Wave angle	θ	°	0 (head sea)

Table 2. Properties of materials used in model

Material	Young's modulus, E, (GPa)	Poisson's ratio, ν	Density, ρ, kg/m^3	Thickness, h_f (h_c), mm
Facing materials:				
LDPE	0.28	0.49	900	10.22 (369.56)
HDPE	1	0.45	950	10.00 (370.00)
Acryl	3.1	0.35	1120	8.45 (373.10)
FRP	12	0.33	1700	5.53 (378.95)
HPC*	40	0.18	2450	3.82*(382.36)
Aluminum	70.3	0.35	2700	3.46 (383.08)
Steel	210	0.33	7800	1.20 (387.60)
Core material:				
Polystyrene foam/Styrofoam™	0.015	0.20	24	

**The small thickness of HPC facing is adopted for comparison purpose, in practical scenario, the thickness has to be larger than 5mm.*

The floating jetty is a rectangular pontoon composed of hollow HDPE (High Density Polyethylene) blocks of dimensions 483×483×390mm which are connected using pin joints (according to Versadock International & Jet Dock Systems). In the analysis, the jetty is modeled as a sandwich structure that is divided into 340 strips and connected at 0.483m intervals along the length. The top and bottom facings of the plate may be assumed to be either LDPE (low density polyethylene), or HDPE (high density polyethylene), or acrylic glass, or FRP (fibre reinforced plastic), or HPC (high performance concrete), or aluminum, or steel. The core can be hollow or filled with light materials like polystyrene foam which has a high resistance to water penetration and can be easily bonded. The jetty is assumed to be fixed in position by mooring lines which restrain its movement in y-direction, i.e. sway. Particulars of the floating plate model, sea states and properties of materials used in this study are listed in Tables 1 and 2, respectively. The water waves adhere to the steepness ratios, i.e. $(2A/\lambda) < 0.17$ and $2A < 0.8H$, and so the waves do not break.

3.1. Response of Krabi floating jetty

Based on present studies, the floating jetty is best modeled as a sandwich plate with semi-rigid line

connectors (ζ_r = 6). Figure 3 compares the simulated response with the actual response of the floating jetty. It is assumed that the front (x/L = 1) and back (x/L = 0) ends of the jetty are restricted to move in the vertical plane, i.e. the model is assumed to be fixed at both ends. It can be seen that, in general, the simulated response agrees well with the actual ones.

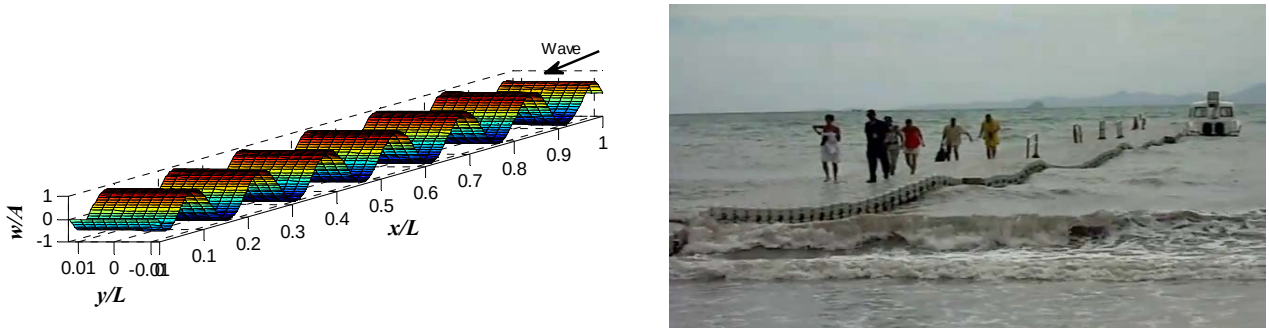

Figure 3: Simulated and actual responses of Krabi floating jetty.

The influence of boundary condition on the response of the floating jetty is also studied by removing the constraint at the front end of the jetty, thereby making the jetty free at its front end and fixed at its back end. As shown in Fig. 4, the responses of the jetty with two types of boundary conditions are almost the same in general, except at the front end. This indicates that the front end boundary condition has a minimal effect on the overall response of the longish floating jetty.

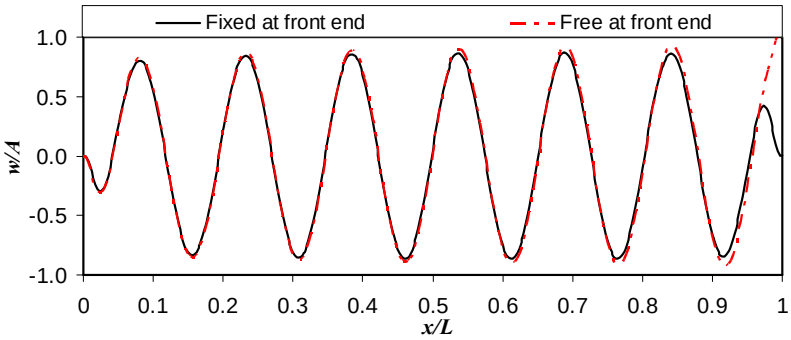

Figure 4: Response of floating jetty with different boundary conditions at front end (x/L = 1).

3.2. Effect of different facing materials

The effect of facing materials on the hydroelastic behavior of floating plate is studied by changing the thickness of the facings while keeping constant the total mass 18290 kg and total height 0.390m of the floating jetty. First, the responses of a continuous (without connectors) plate with different facing materials are investigated. As shown in Fig. 5, the hydroelastic response (deflection parameter Ψ and maximum displacement w_{max}/A) of floating plate largely depends on its flexural rigidity. As its flexural rigidity increases, the response of the jetty decreases. Among all the materials considered, steel facings (which have the higher flexural rigidity) produces the minimum values for both Ψ and w_{max}/A. The associated centerline (y = 0) responses of a continuous (with ζ_r = 600) jetty with HDPE, FRP, and steel facings are also shown in Fig. 7a.

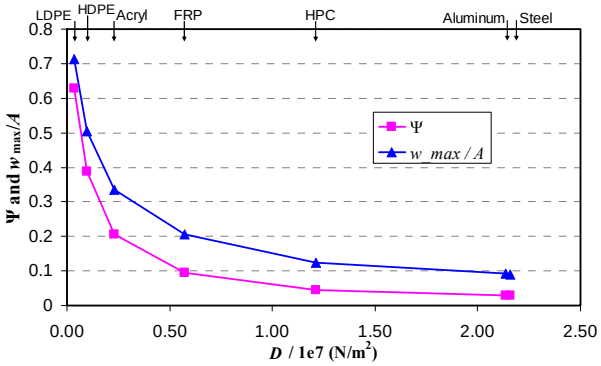

Figure 5: Effect of facing materials on the response of a continuous floating jetty.

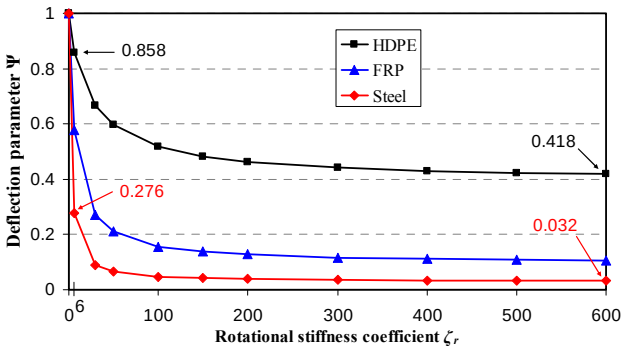

Figure 6: Effect of rotational stiffness of connectors on the response of the jetty.

3.3. Effect of rotational stiffness of connector

The effect of rotational stiffness of the line connectors on the hydroelastic response of the floating jetty are investigated by varying the coefficient of rotational stiffness of the line connectors. Three different facing materials are considered, i.e. HDPE, FRP, and Steel. Figure 6 shows the variations of Ψ with respect to the coefficient ζ_r of rotational stiffness of the line connectors. It can be seen that the response parameter drops as the rotational stiffness increases. When ζ_r = 600, the floating jetty almost becomes a rigid (or continuous) plate. On the other hand, when ζ_r approaches 0, Ψ approaches unity which suggests that the response profile of the floating jetty becomes exactly the same as the incoming plane wave profile, irrespective of the facing material chosen (see Fig. 7c). This is because the floating jetty now behaves as a pin-connected structure with 340 modules and each module is dominated by rigid body motion due to its small length (0.483m).

It is clear from Fig. 6 that in terms of Ψ, the response of Krabi jetty (ζ_r = 6) with HDPE facings can be reduced by using more rigid connections (say ζ_r = 600). Note that Ψ is reduced by about one half (from 0.858 to 0.418). Also, by using a more rigid facing material like steel, Ψ can be reduced by 68% (from 0.858 to 0.276). By combining the use of rigid connections and steel facings, the response Ψ can be reduced significantly (from 0.858 to 0.032).

4. CONCLUSIONS

We have studied the hydroelastic behavior of Krabi floating jetty under wave action. Investigated herein are the effects of using different facing materials and rotational stiffness of the line connectors on the hydroelastic response of Krabi floating jetty that is modeled by a longish equivalent sandwiched plate. It is found that by using a facing material of higher flexural rigidity, one can reduce the response of the flexible jetty. Steel is found to be the most effective among the facing materials considered. Also, rigid line connectors results in smaller responses. By combining the use of rigid connections and materials with higher flexural rigidity, the response of Krabi jetty can be reduced significantly.

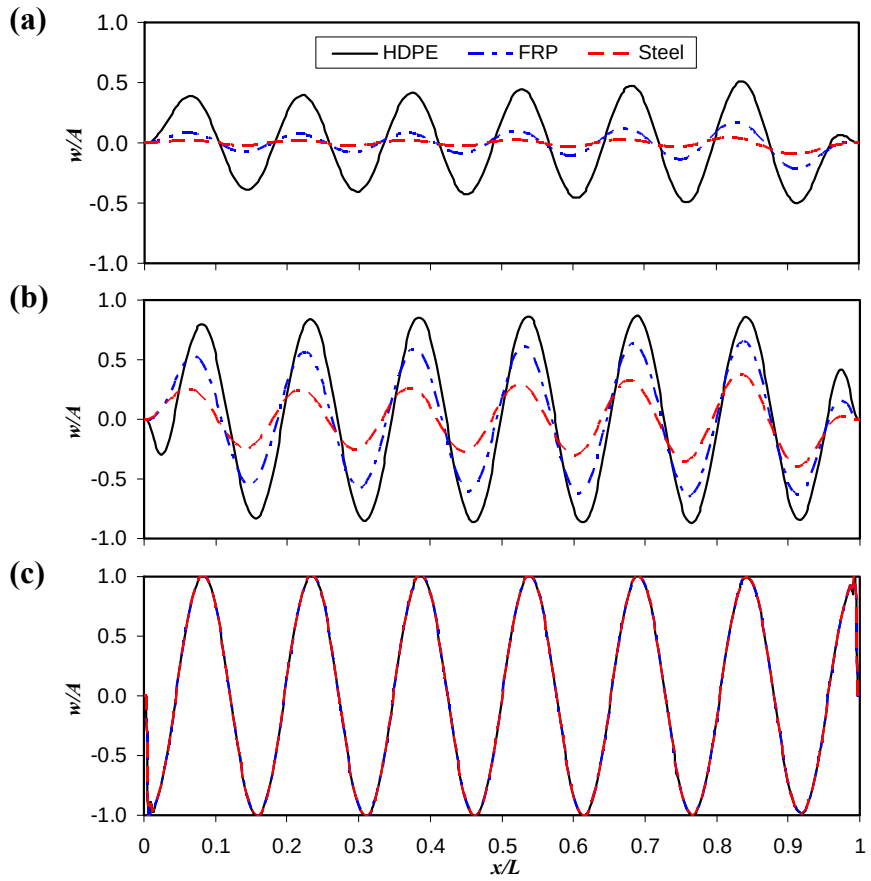

Figure 7: Responses of floating jetty with different facings. (a) $\zeta_r = 600$, (b) $\zeta_r = 6$ and (c) $\zeta_r = 0$.

5. ACKNOWLEDGMENTS

The authors would like to thank the Thai Meteorological Department for providing the wave data and Versadock International and Jet Dock Systems for providing the details of the jetty design.

REFERENCES

Eatock Taylor, R and Waite, JB (1978). The dynamics of offshore structures evaluated by boundary integral techniques. International Journal for Numerical Methods in Engineering. 13(1), pp. 73-92.

Gao, RP, Tay, ZY, Wang, CM and Koh, CG (2011). Hydroelastic response of very large floating structure with a flexible line connection. Ocean Engineering. 38(17-18), pp. 1957-1966.

Lee, CH and Newman, JN (2000). An assessment of hydroelasticity for very large hinged vessels. Journal of Fluids and Structures. 14(7), pp. 957-970.

Liew, KM, Wang, CM, Xiang, Y and Kitipornchai, S (1998). Vibration of Mindlin Plates: Programming the p-version Ritz Method. Oxford, UK, Elsevier.

Linton, CM (1999). Rapidly convergent representations for green's functions for Laplace's Equation. Proceedings of the Royal Society of London. Series A: Mathematical, Physical and Engineering Sciences. 455(1985), pp. 1767-1797.

Newman, JN (1994). Wave effects on deformable bodies. Applied Ocean Research. 16(1), pp. 47-59.

Sarpkaya, T and Isaacson, M (1981). Mechanics of Wave Forces on Offshore Structures. New York, Van Nostrand Reinhold Co.

Savannah, R. (2011). Not safe pier – Krabi Thailand. Available from: http://www.youtube.com/watch?v=tryJjIWTsPQ.

Versadock Intl ltd. Available from: http://www.versadock.com/products.htm.

Jetdock Systems, Inc. Available from: http://www.jetdock.com/products/conventional-floating-walkway.asp.

Wang, CM, Watanabe, E and Utsunomiya, T (2008). Very Large Floating Structures. Abingdon, UK, Taylor & Francis.